

Scholar Journal of Applied Sciences and Research

Analysis of Motions for Gyroscope with One Side Support

Ryspek Usubamatov^{1*}

¹Faculty of Transport and Manufacturing Engineering, Kyrgyz State Technical University, Kyrgyzstan

Abstract

Contemporary engineering widely uses the gyroscopes, which are main units for navigation and control systems work on a principle of maintaining the axis of a spinning rotor in a space. This gyroscope property formulated by mathematical models based on Euler's the principle of the change in the angular momentum. Nevertheless, the actual acting forces and motions of the gyroscopes do not match theoretical approach. This circumstance commits researchers to find true mathematical solutions. New research results in the area of gyroscopic devices have demonstrated that the gyroscope effects have an origin that is more complex than presented in publications. Investigations manifested that rotating mass of the gyroscopes generates several inertial torques based on the action of the centrifugal, common inertial and Coriolis forces as well as the change in the angular momentum. These torques are interrelated and acted at one time around two gyroscope axes, and represented the internal resistance and precession torques. Practically, the gyroscopic devices run with the action of the frictional forces on the supports and pivots that have the effect upon on gyroscope motions. This work represents an analytic solution for motions of the gyroscope with one side support based on the action of the load, internal and frictional torques. A mathematical model for the gyroscope motions under the action of the external and internal torques is validated by practical tests.

Keywords: Gyroscope, Theory, Property, Test, Torque.

Introduction

More than two centuries ago famous mathematician L. Euler first lay out the mathematical foundations for the gyroscope theory in his work on the dynamics of rigid bodies. At those time other brilliant scientists such as I. Newton, J-L. Lagrange, L. Poinsot, J.L.R. D'Alembert, P-S. Laplace, L. Foucault, and others analyzed and interpreted the gyroscope property of maintaining the axis of a spinning rotor in a space. The industrial revolution and following engineering activity in the twentieth century developed the applied theory of gyroscopic devices and systems [1-5]. Since those times, probably tons of manuscripts and several dozens of gyroscope theories were published. These publications explain the gyroscope effects in terms of the conservation of kinetic energy and by the action of the change in the angular momentum of the spinning rotor.

Today, gyroscopic devices are primary units for navigation and control systems that are widely used in engineering industries [6,7]. The textbooks of classical mechanics contain the chapters dedicated to the gyroscope theory [8-10]. Nevertheless, the known textbooks and manuscripts do not explain fully and adequately the physics of acting

Article Information

Article Type: Review

Article Number: SJASR 133

Received Date: 28 May, 2018

Accepted Date: 20 June, 2018

Published Date: 3 July, 2018

***Corresponding author:** Dr. Ryspek Usubamatov, Professor, Faculty of Transport and Manufacturing Engineering, Kyrgyz State Technical University, Kyrgyzstan. Tel: + 996-312-298834; Email: ryspek0701@yahoo.com

Citation: Usubamatov R (2018) Analysis of Motions for Gyroscope with One Side Support. Sch J Appl Sci Res. Vol: 1, Issu: 4 (5 - 13).

Copyright: © 2018 Usubamatov R. This is an open-access article distributed under the terms of the Creative Commons Attribution License, which permits unrestricted use, distribution, and reproduction in any medium, provided the original author and source are credited.

forces on the gyroscope and its motions in a space [11,12].

For practical application, the forces and motions of gyroscopes formulated by severe numerical mathematics based on Lagrangian dynamics that is solved with computer's software [13]. These theories and other publications explain gyroscope effects based on deductions, assumptions and simplifications [14-16]. Unexplained gyroscopic effects, researchers intuitively pointed on the action of the inertial forces of the rotating disc. Nevertheless, this true intuition did not formulate the mathematical models of the action of inertial forces on a gyroscope, except only the principle of the change in the angular momentum [17,18]. From this, researchers created several artificial terms like gyroscope resistance, gyroscope effects, gyroscope couple, and so on that contradict known terms of classical mechanics. These unsolved gyroscope problems have represented the challenge for researchers to formulate the mathematical models for acting forces and motions for gyroscopic devices [19,20].

New investigations of the physical principles of gyroscopic devices demonstrate that the origin of gyroscope properties and effects is more complex than seemed. The inertial forces generated by the spinning mass elements and center mass of the rotor, produce the several torques based on the action of centrifugal, common inertial and Coriolis forces as well as changes in the angular momentum. The mathematical models and physical principles of these inertial torques are well described and present the basis for all gyroscope effects and properties [21].

New analytical investigations of the gyroscope's internal torques demonstrate that the actions of them are interrelated and occur simultaneously around two gyroscope axes. The action of the change in the angular momentum represents the small component in gyroscope properties. The results of new studies make clear why the known gyroscope theories contain too many simplifications and assumptions.

New mathematical models for gyroscope motions accurately describe gyroscope effects. Moreover, these models discover new gyroscope properties and interpret known one. The basic mathematical models for motions of the gyroscope validated by practical tests that conducted on Super Precision Gyroscope (Brightfusion Ltd, Abbeymead, UK). These new fundamental principles for gyroscope theory can solve all gyroscope problems and represent new challenges for future studies of gyroscopic devices [22-25].

In engineering, most of these gyroscopic devices run with the frictional forces that are results of the action of external and internal torques on the supports and pivots. The frictional torques are external ones, which values can be commensurable with the values of the resulting torques acting on the gyroscope. Practice demonstrates the frictional forces have an effect upon on gyroscope motions, which velocities of rotation around axes in increased. At first sight, this phenomenon of the gyroscope motions contradicts to the rules of classical mechanics that state the velocity of the object decreases with the action of the frictional force. This work represents a mathematical model for motions of a gyroscope with one side support under the action of the

external and internal torques, and explain the physics of the unusual properties.

Methodology

Recent analytic investigations of the gyroscope motions have presented new mathematical models of inertial forces acting in a gyroscope. The action of the external load on a gyroscope generates several inertial resistance and precession torques, whose physics well described and represented in (Table 1), [23]. Research demonstrated that the centrifugal and Coriolis forces generated by the mass elements of the spinning rotor produce the resistance torque. The common inertial forces and the change in the angular momentum generate the precession torque. This resistance and precession torques act perpendicular to each other around their axes and simultaneously interrelated [13]. The action of the load and inertial torques on the supports and pivots of the gyroscopes generate the frictional forces. The frictional torques are considered the external load that has an appreciable influence on the motions of gyroscopic devices.

Table 1 contains the several symbols that marked by subscript signs indicating the axis of action, where for instance T_{rx} is the resistance torque acting around axis ox , ω_y is the angular velocity of precession around axis oy , etc., J is the mass moment of inertia of the gyroscope's rotor around the axle. ω_i is the angular velocity of the gyroscope around axis i and ω is the angular velocity of a spinning rotor.

Mathematical models for motions of the gyroscope with one side support consider the interrelated action of external and inertial torques on the supports and pivot around two axes. The values of any external torques generate proportionally the values of inertial one acting around two axes. The action of the internal torques around axes expresses the internal kinetic energies of the spinning rotor that are equal along axes [23]. Hence, any change in the value of the internal torques around one axis leads to the reciprocal change in the value of the internal torques around another axis. The analytic models for the motions of the gyroscope are considered on a stand represented in (Figure 1). A detailed picture of the gyroscope's stand and its geometrical parameters is shown in (Figure 2). Technical data of the test stand with Super Precision Gyroscope, "Bright fusion LTD" is represented in (Table 2).

Table 1: Internal torques acting on a gyroscope.

Torque generated by	Equation, (N.m)
Centrifugal forces, $T_{cl.i}$	$T_{ct.i} = T_{in.i} = 2\left(\frac{\pi}{3}\right)^2 J\omega_i$
Inertial forces, $T_{in.i}$	
Coriolis forces, $T_{cr.i}$	$T_{cr.i} = (8/9)J\omega_i$
Change in angular momentum, $T_{am.i}$	$T_{am.i} = J\omega_i$
Resistance torque $T_{r.i} = T_{cl.i} + T_{cr.i}$	$T_{r.i} = \left[2\left(\frac{\pi}{3}\right)^2 + \frac{8}{9}\right]J\omega_i$
Precession torque $T_{p.i} = T_{in.i} + T_{am.i}$	$T_{p.i} = \left[2\left(\frac{\pi}{3}\right)^2 + 1\right]J\omega_i$



Figure 1: The stand of the gyroscope with one side support.

Table 2 contains the following symbols: $J_x = J_y = (MR^2/4) + Ml^2$ is the mass moment of the gyroscope's inertia around axes ox and oy respectively; R is the external radius of the gyroscope; l is the overhang of the centre of gravity of the gyroscope from the centre beam; M is the mass of the gyroscope; $J_{rx} = J_{ry} = (m_r R_c^2/4)$ is rotor's mass moment of inertia around axis ox and oy ; R_c is the conditional radius of the rotor; $J = (m_r R_c^2/2)$ is rotor's mass moment of inertia around axis oz . m_f is the mass of the gyroscope's frame; r_f is the radius of the frame; The computed mass moments of the gyroscope's components inertia around axes ox and oy is presented in [23].

The gyroscope was assembled on the centre beam b with the ability freely rotate around axis ox on the spherical journals of sliding bearings B and D . The centre beam b is located on the two vertical arms of the frame, which is assembled on horizontal bar b_s (Figures 1 and 2). The bar has the ability to rotate around the pivot C (axis oy) on the platform.

The mathematical model of motions for the gyroscope with one side support is formulated for the common case when its axle is inclined on the angle γ . The basis of this model is described in [23] and used with the modification that includes the action of the frictional torques on the supports and pivot. The change in the values of the external and inertial torques is expressed by the correction coefficient η .

The action of the frictional torques around axes ox and oy decreases the values of the torque generated by the gyroscope weight and the precession torques respectively. The resistance torques acting around axis oy are depended on the precession torques. Hence, the value of the inertial torques acting around axis ox also is decreased proportionally. The changes in values of inertial torques acting around two axes are equal because the inertial torques are expressed the inertial kinetic energies of the spinning rotor that are equal along axes. Then, the mathematical models for motions of the gyroscope are represented by the following Euler's differential equations:

$$J_{Ex} \frac{d\omega_x}{dt} = T \cos \gamma + T_{x.ct.y} - T_{f.x} - (T_{ct.x} + T_{cr.x} + T_{in.y} \cos \gamma + T_{am.y} \cos \gamma) \eta \quad (1)$$

$$J_{Ey} \frac{d\omega_y}{dt} = (T_{in.x} \cos \gamma + T_{am.x} \cos \gamma - T_{ct.y} \cos \gamma - T_{cr.y} \cos \gamma) \eta - T_{y.cr.y} - T_{f.y} \quad (2)$$

$$\omega_y = - \left(\frac{2\pi^2 + 8}{\cos \gamma} + 2\pi^2 + 9 \right) \omega_x \quad (3)$$

where ω_x and ω_y is the angular velocity of the gyroscope around axes ox and oy , respectively; $T_{ct.x}$, $T_{ct.y}$, $T_{cr.x}$, $T_{cr.y}$, $T_{in.x}$, $T_{in.y}$, $T_{am.x}$ and $T_{am.y}$ are inertial torques generated by the centrifugal, Coriolis, inertial forces and the change in the angular momentum acting around axes ox and oy , respectively (Table 1); η is the coefficient of the decreasing of the inertial torques due to the action of the frictional torques on gyroscope's pivot; other components are as specified above.

Analysis of the torques acting on the gyroscope demonstrates the following peculiarities. The external load torque T that is produced by the gyroscope weight W generates the frictional and inertial torques acting around axes ox and oy (Figure 2). These torques are represented by the following components:

- a) The resistance torques generated by the centrifugal forces $T_{ct.x}$ and Coriolis forces $T_{cr.x}$ acting around axis ox ;
- b) The procession torques generated by the inertial forces $T_{in.x}$ and the change in the angular momentum $T_{am.x}$ acting around axis oy .
- c) The procession torques $T_{in.x}$ and $T_{am.x}$ in turn generate the resistance torques of centrifugal forces $T_{ct.y}$ and of Coriolis forces $T_{cr.y}$ acting around axis oy , respectively.
- d) The resulting torque acting around axis oy , in turn, generates the procession torques of inertial forces $T_{in.y}$ and the change in angular momentum $T_{am.y}$ acting around axis ox ;
- e) The gyroscope weight produces the external frictional torques $T_{f.W.x}$ and $T_{f.W.y}$ acting around axes ox and oy , respectively.
- f) The rotation of the gyroscope around axes ox and oy generates the centrifugal forces of the gyroscope centre mass $F_{y.ct.x}$ and $F_{y.ct.y}$ that produce the frictional torques $T_{f.ct.x}$ and $T_{f.ct.y}$ acting around axes ox and oy on the supports, respectively.
- g) The rotation of the gyroscope around axes oy and ox generates the Coriolis force of the gyroscope centre mass that produce the torques $T_{f.x.cr.y}$ acting around axes ox and oy on the supports and pivot, respectively.

The peculiarity of the action of the gyroscope's inertial torques is as follows:

- 1) The frictional torques acting around axis ox are adding acting to inertial torques;
- 2) The procession torques acting around axis oy generate the resistance torques acting in opposite direction. The frictional torques acting around axis oy decrease the value of the procession torques.
- 3) Changes in the value of the inertial torque acting around axis oy lead to the change in the value of the inertial torques acting around axis ox .

Table 2: Technical data of the test stand with Super Precision Gyroscope, “Brightfusion LTD”.

Parameters	Mass, kg	Mass moment of inertia around axis ox and oy , J kg.m ²
Spinning rotor with shaft, m_r	0.1159	$J = m_r R^2 / 2 = 0.5726674 \times 10^{-4}$ (around axis oz)
Gyroscope, M	0.146	$J_{IM} = (2/3)m_r r_f^2 + m_f^2 + (m_r R_c^2 / 4) + m_r^2 = 2.284736 \times 10^{-4}$
Centre beam with journals and screw, b	0.028	$J_{bx} = m_b r_b^2 / 2 = 0.00224 \times 10^{-4}$ (around axis ox)
Mass $E = M + b$	0.174	$J_{by} = m_b^2 / 12 = 0.2105833 \times 10^{-4}$ (around axis oy)
Bar with screws, b_s	0.067	$J_{Ex} = J_{xM} + J_{bx} = 2.286976 \times 10^{-4}$ (around axis ox)
Arm, a	$2 \times 0.009 = 0.018$	$J_{Ey} = J_{xM} + J_{by} = 2.495319 \times 10^{-4}$ (around axis ox)
Total	0.259	$J_{bx} = m_{bs}^2 / 12 = 0.51456 \times 10^{-4}$ (around axis oy)
$A = M + b + b_s + a$		$J_a = m_r^2 / 2 + m_a I_a^2 = 0.41553 \times 10^{-4}$ (around axis oy)
		$J_y = J_{yM} + J_b + J_{bs} + J_a = 3.38437 \times 10^{-4}$ (around axis oy)

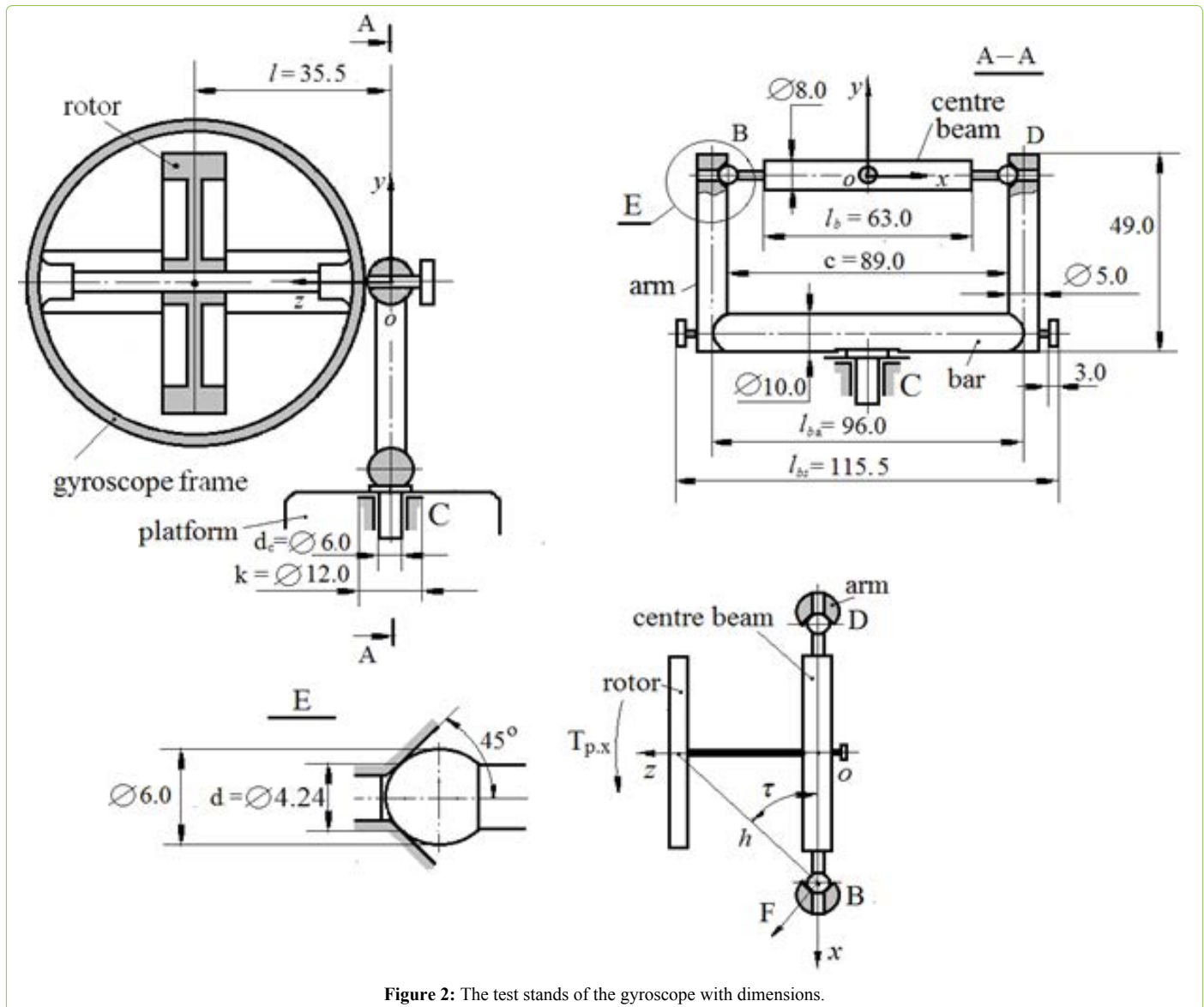


Figure 2: The test stands of the gyroscope with dimensions.

The running gyroscope produces several external and inertial torques acting around two axes that are expressed by the following equations:

(a) The weight of the gyroscope inclined on the angle γ produces the torque T acting around axis ox in the counter clockwise direction:

$$T = Mgl \quad (4)$$

where M is the gyroscope mass; g is the gravity

acceleration, l is the distance between the centre mass of the gyroscope and axis of the centre beam (Figure 2), γ is the angle of the axle inclination.

(b) The torque generated by the centrifugal force of the rotating gyroscope centre mass around axis oy acting in the counter clockwise direction around axis ox :

$$T_{x.ct.y} = Ml(\cos \gamma)\omega_y^2(l \sin \gamma) = Ml^2 \omega_y^2 \cos \gamma \sin \gamma \quad (5)$$

where ω_y is the angular velocity of the gyroscope around axis oy and other components are as specified above.

(c) The centrifugal force of the rotating gyroscope centre mass around axis ox acting along axis oz (Figure 2)

$$F_{z.ct.x} = Ml\omega_x^2 \tag{6}$$

where ω_x is the angular velocity of the gyroscope around axis ox and other components are as specified above.

(d) The frictional torques acting on the supports B and D is represented by the following equation:

$$T_{f.x} = T_{f.x.E.x} + T_{f.x.cr.y} + T_{f.z.ct.x} + T_{f.x.ct.y} \tag{7}$$

Where:

(e) The frictional torque acting on the supports B and D (Fig. 2) in the clockwise direction around axis ox generated by the centrifugal force of the rotating gyroscope centre mass around axis oy :

$$T_{f.x.ct.y} = Ml\omega_y^2 \cos \gamma \left(\frac{df}{2 \cos \delta} \right) \tag{8}$$

where d is the diameter of the centre beam, f is the frictional sliding coefficient, $\delta = 45^\circ$ is the angle of the cone of sliding bearing of the supports (Figure 2) and other components are as specified above.

(f) The frictional torque acting on the supports B and D in the clockwise direction around axis ox generated by the centrifugal force of the rotating gyroscope centre mass around axis ox :

$$T_{f.z.ct.x} = Ml\omega_x^2 \frac{df}{2 \cos \delta} \tag{9}$$

where all components are as specified above.

(g) The frictional torque acting on the supports B and D in the clockwise direction around axis ox generated by the Coriolis force of the rotating gyroscope centre mass around axes oy and ox :

$$T_{f.x.cr.y} = Ml\omega_y\omega_x \sin \gamma \left[\frac{l}{h} \frac{df}{2 \cos(\delta - \tau)} \right] \tag{10}$$

where $h = 56.925$ mm is the distance between the centre of the gyroscope and the support (Figure 2); $\tau = \arctan (l/[c/2]) = 38.581^\circ$ is the angle of the action of Coriolis force on the sliding bearing and other components are as specified above.

(h) The frictional torque acting on the sliding bearing of the supports B and D in the clockwise direction around axis ox generated by the gyroscope weight with the centre beam E :

$$T_{f.x.cr.y} = Ml\omega_y\omega_x \sin \gamma \left[\frac{l}{h} \frac{df}{2 \cos(\delta - \tau)} \right] \tag{11}$$

where E is the mass of the gyroscope with the centre beam (Table 2), $F_{y.ct.x} = Ml\omega_x^2 \sin \gamma$ is the centrifugal force of the rotating gyroscope centre mass around axis ox acting along axis oy (Figure 2) and other components are as specified above.

The expression of the total frictional torque (Equations (8)-(11)) acting on the supports B and D is represented by

the following equation:

$$T_{f.x} = (Eg - Ml\omega_x^2 \sin \gamma) \frac{df}{2 \cos \delta} + Ml\omega_y\omega_x (\sin \gamma) \frac{l}{h} \frac{df}{2 \cos(\delta - \tau)} + Ml\omega_x^2 \frac{df}{2 \cos \delta} + Ml\omega_y^2 (\cos \gamma \sin \gamma) \frac{df}{2 \cos \delta} \tag{12}$$

The torque generated by Coriolis force of the rotating gyroscope centre mass around axes oy and ox , and acting in the clockwise direction around axis oy :

$$T_{y.cr.y} = (Ml\omega_y \sin \gamma)(\omega_x l \sin \gamma) = M\omega_y\omega_x (l \sin \gamma)^2 \tag{13}$$

where all components are as specified above.

The frictional torques acting on the pivot C is represented by the following equation:

$$T_{f.y} = T_{f.y.F.y} + T_{f.y.cr.y} + T_{f.y.ct.y} + T_{f.z.ct.x} \tag{14}$$

Where:

(j) The frictional torque acting on the pivot C (Fig. 2) in the clockwise direction generated by the centrifugal force of the rotating gyroscope centre mass around axis oy :

$$T_{f.y.ct.y} = Ml\omega_y^2 \cos \gamma \left(\frac{d_c f_c}{2} \right) \tag{15}$$

where d_c is the diameter of the pivot; f_c is the frictional sliding coefficient and other components are as specified above.

(k) The frictional torque acting on the pivot C in the clockwise direction around axis oy generated by the centrifugal force of the rotating gyroscope centre mass around axis ox and acting along axis oz :

$$T_{f.z.ct.x} = Ml\omega_x^2 \cos \gamma \left(\frac{d_c f_c}{2} \right) \tag{16}$$

where all components are as specified above.

(l) The frictional torque acting on the pivot C generated by Coriolis force of the rotating gyroscope centre mass around axes oy and ox :

$$T_{f.y.cr.y} = Ml\omega_y\omega_x \sin \gamma \left(\frac{d_c f_c}{2} \right) \tag{17}$$

where all components are as specified above.

(m) The frictional torque acting on the thrust sliding bearing of the pivot C in the clockwise direction around axis oy produced by the gyroscope's stand and the centrifugal force of the centre mass rotating around axis ox :

$$T_{f.y.F.y} = (Ag - Ml\omega_x^2 \sin \gamma) \left(\frac{k - d_c}{4} + \frac{d_c}{2} \right) f_c \tag{18}$$

where A is the total mass of the gyroscope stand (Table 2); k is the external diameter of the thrust sliding bearing of the pivot C , $Ml\omega_x^2 \sin \gamma$ is the centrifugal force of the rotating gyroscope centre mass around axis ox and acting along axis oy , other components are as specified above.

The expression of the total frictional torques (Equations (15)-(18)) acting on the pivot C is represented by the following equation: v

$$T_{f.y} = (Ag - Ml\omega_x^2 \sin \gamma) \left(\frac{k - d_c}{4} + \frac{d_c}{2} \right) f_c + \tag{19}$$

$Ml(\sin \gamma)\omega_y\omega_x \frac{d_c f_c}{2} + Ml\omega_x^2 (\cos \gamma) \frac{d_c f_c}{2} + Ml\omega_y^2 (\cos \gamma)\omega_x^2 \frac{d_c f_c}{2}$ (Figure 3) represents the scheme of the gyroscope stand with the action of external and internal torques.

Analysis of the action of the external and inertial torques enables the physical principles of the gyroscope motions around axes to be formulated. The following gyroscope properties that were obtained by practical tests are used for the mathematical models of the gyroscope motions with the action of the frictional torques:

a) The action of the frictional torques on the supports around axis *ox* of the gyroscope leads to the decreasing of the value of the torque generated by the gyroscope weight. In turn, this leads to decreasing the value of inertial torques acting around axis *ox* and *oy*.

b) The action of the frictional torques on the pivot around axis *oy* of the gyroscope leads to the decreasing of values of the inertial precession torques generated by the torques acting around axis *ox*.

c) The resulting torques acting around axes generate minor reactions of second order on the supports and pivot that can be neglected [23-26].

d) The value of the frictional torques acting on supports and pivot is commensurable with the value of the resulting inertial torques acting on the gyroscope.

The presented properties are important for the mathematical modelling of motions of the gyroscope with one side support around two axes. The mathematical model for gyroscope motions under the action of the external and inertial torques validated by the practical tests. The test results recorded the values of the time for the gyroscope rotating around axes *ox* and *oy*.

The tests of the gyroscope motion demonstrated that the angular velocities of gyroscope's rotation around axes *ox* and *oy* are bigger than for its motion without the action of the frictional torques. At first sight, this gyroscope property contradicts to rules of classical mechanics. However, analysis of the acting torques and motions of the gyroscope enables this property to be explained by the following reason. The action of the frictional torques decreases the values of inertial torques that lead to increasing the action of the load torque. This peculiarity is expressed by the coefficients of the change in the values of the gyroscope inertial torques.

The technical data of the gyroscope stand, which are represented in Table 2 and Figure 2,3 enable the following information to be used for mathematical modelling of the gyroscope motions.

The gyroscope standard (Figure 2) generates the frictional torques acting around axes *ox* and *oy*. The correction coefficient η for the internal torques is considered for the frictional torques T_{fy} only acting around axis *oy*. The reason is the precession torques acting around axis *oy* is the load torque that depends on torques acting around axis *ox*. The frictional torques acting around axis *oy* decrease the value of the precession torques. The frictional torques acting around axis *ox* decrease the value of the load torque that produces the dependent inertial torques. From this,

it followed that the coefficient η expresses the mutual, reciprocal and interrelated action of two frictional torques acting around two axes. The frictional torques acting around axis *ox* is part of the load torque that generates the precession torques acting around axis *oy*. Hence, the coefficient η is expressed by the ratio of the difference between the precession torques $(T_{inx} + T_{amx}) \cos \gamma$ and the frictional torque T_{fy} , to the precession torques acting around axis *oy*. Substituting equations of Table 1 and Equations (13) and (19) into the ratio of these torques and transformation yields the expression of correction coefficient η

$$\eta_{x,y} = \frac{(T_{inx} + T_{amx}) \cos \gamma - T_{y,cr,y} - T_{f,y}}{(T_{inx} + T_{amx}) \cos \gamma} = 1 - \frac{T_{y,cr,y} + T_{f,y}}{(T_{inx} + T_{amx}) \cos \gamma} =$$

$$1 - \frac{\left[M\omega_x \omega_x (l \sin \gamma)^2 + (Ag - Ml\omega_x^2 \sin \gamma) \left(\frac{k-d_c}{4} + \frac{d_c}{2} \right) f_c + Ml\omega_x \omega_x (\sin \gamma) \frac{d_c f_c}{2} + \right.}{\left. Ml\omega_x^2 (\cos \gamma) \frac{d_c f_c}{2} + Ml\omega_y^2 (\cos \gamma) \frac{d_c f_c}{2} \right]}{\left[2 \left(\frac{\pi}{3} \right)^2 + 1 \right] J\omega_x \cos \gamma} \quad (20)$$

where η is the coefficient of correction for the action of two frictional torques around two axes *ox* and *oy*; other components are as specified above.

Analysis of Equation (20) enables for demonstrating the following results. In case of absence of the frictional torques T_{fy} acting around axes *oy*, means that the value of correction coefficient of $\eta = 1.0$. In case, when the frictional torques T_{fy} are equal to the precession torques T_{px} acting around axes *oy*, means that the value of correction coefficient of $\eta = 0$. The gyroscope does not turn around axis *oy* and inertial torques of axis *ox* are deactivated. This fact is validated by practical tests.

Substituting defined equations for the internal torques of the gyroscope (Table 1), Equations (4)-(6), (12), and (13) into Equations (1) and (2) yields the following system of differential equations:

$$J_{Ex} \frac{d\omega_x}{dt} = Mgl \cos \gamma + Ml^2 \omega_y^2 \cos \gamma \sin \gamma -$$

$$\left[\frac{Eg}{2 \cos \delta} \frac{df}{d\delta} + Ml\omega_x \omega_x (\sin \gamma) \frac{l}{h} \frac{df}{2 \cos(\delta - \tau)} + Ml\omega_x^2 \frac{df}{2 \cos \delta} + Ml\omega_y^2 (\cos \gamma \sin \gamma) \frac{df}{2 \cos \delta} \right] -$$

$$\left[2 \left(\frac{\pi}{3} \right)^2 J\omega_x + \frac{8}{9} J\omega_x + 2 \left(\frac{\pi}{3} \right)^2 J\omega_y \cos \gamma + J\omega_y \cos \gamma \right] \eta \quad (21)$$

$$J_{Ey} \frac{d\omega_y}{dt} = \left[2 \left(\frac{\pi}{3} \right)^2 J\omega_x \cos \gamma + J\omega_x \cos \gamma - 2 \left(\frac{\pi}{3} \right)^2 J\omega_y \cos \gamma - \frac{8}{9} J\omega_y \cos \gamma \right] \eta -$$

$$M\omega_x \omega_x (l \sin \gamma)^2 - (Ag - Ml\omega_x^2 \sin \gamma) \left(\frac{k-d_c}{4} + \frac{d_c}{2} \right) f_c + Ml\omega_x \omega_x (\sin \gamma) \frac{d_c f_c}{2} +$$

$$Ml\omega_x^2 (\cos \gamma) \frac{d_c f_c}{2} + Ml\omega_y^2 (\cos \gamma) \frac{d_c f_c}{2} \quad (22)$$

where all components are as specified above.

Following solution of Equations (21) and (22) is the same that presented in [23]. Substituting Equations (20) into equations Equations (21) and (22) yields the following equation:

Table 3: Experimental and theoretical results of the gyroscope precessions.

Gyroscope average parameters	Tests	Theoretical	Difference, %
Time of one precession revolution around axis oy , s	3.7	3.385	9.3
Time of precession of the gyroscope motion around axis ox on 20° (from $+10^\circ$ to -10°) of the turnabout horizontal location around axis ox , s	11.5	10.626	8.2

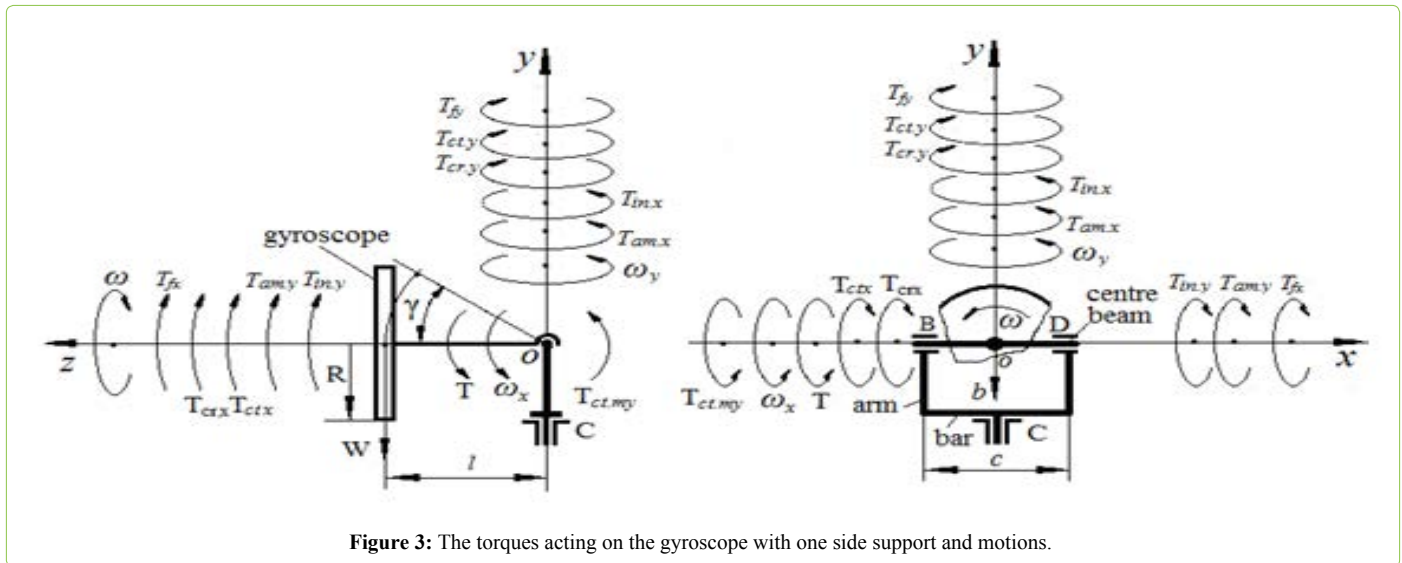


Figure 3: The torques acting on the gyroscope with one side support and motions.

$$\begin{aligned}
 J_{Ex} \frac{d\omega_x}{dt} &= Mgl \cos \gamma + Ml^2 \omega_x^2 \cos \gamma \sin \gamma - \\
 &\left[\frac{Eg}{2 \cos \delta} \frac{df}{dh} + Ml \omega_x \omega_y (\sin \gamma) \frac{l}{h} \frac{df}{2 \cos(\delta - \tau)} + \right] - [2\pi^2 + 8 + (2\pi^2 + 9) \cos \gamma] J \omega \omega_x \times \\
 &\left[\frac{Ml \omega_x^2 \frac{df}{2 \cos \delta} + Ml \omega_x^2 (\cos \gamma \sin \gamma) \frac{df}{2 \cos \delta}}{2 \left(\frac{\pi}{3} \right)^2 + 1} \right] J \omega \omega_x \cos \gamma
 \end{aligned} \tag{23}$$

Equation (23) is represented the mathematical model for motions of the gyroscope around axis ox with the action of the external and internal torques. For the horizontal location of the gyroscope ($\gamma = 0$), after simplification of Equation (23) and transformation yields the following equation:

$$\begin{aligned}
 J_{Ex} \frac{d\omega_x}{dt} &= Mgl + Ag \frac{9(4\pi^2 + 17)}{2\pi^2 + 9} \left(\frac{k + d_c}{4} \right) f_c - \frac{Egdf}{2 \cos \delta} - (4\pi^2 + 17) J \omega \omega_x + \\
 &\left\{ \frac{9(4\pi^2 + 17) d_c f_c}{2\pi^2 + 9} \frac{1}{2} \left[1 + (4\pi^2 + 17)^2 \right] - \frac{df}{2 \cos \delta} \right\} Ml \omega_x^2
 \end{aligned} \tag{24}$$

where all components are as specified above.

Case Study and Practical Tests

The mathematical model for motions of the gyroscope with one side support is considered on the test stand (Figure 2). For the practical tests is accepted the horizontal location of the gyroscope spinning axle and the action of the frictional torques on the supports and pivot. The coefficients of the sliding friction in supports and pivots defined empirically $f = 0.1$, $f_c = 0.3$. The speed of the gyroscope's rotor for the tests is accepted 10000 rpm. The velocity of the spinning rotor measured by the Optical Multimeter Tachoprobe Model 2108/LSR Compact Instrument Ltd. with range of measurement 0 ... 60,000.00 rpm. The spinning rotor

demonstrated the permanent drop of 67 revolutions per second. The angular measurements of the location for the gyroscope axis were conducted optically by the angular template with accuracy $\pm 1.0^\circ$. The time of the gyroscope motions around axes measured by the stopwatch of Model SKU SW01 with resolution 1/100s.

Results of practical tests are represented by the following average data. The time spent on one revolution around axis oy is $t_y = 3.7$ s, then the angular velocity is $\omega_y = 360^\circ / 3.7$ s = $97.297^\circ / s$. The time spent on the gyroscope turn of 20° around axis ox ($\pm 10^\circ$ about horizontal location) is $t_x = 11.5$ s, then the angular velocity is $\omega_x = 20^\circ / 11.5$ s = $1.739^\circ / s$. Numerical solutions for mathematical models (Equations (1)-(3)) are represented in Appendix. Experimental and theoretical results of the gyroscope precessions around two axes are represented in Table 3.

Analysis of the results of the theoretical calculations and practical tests for the gyroscope precessions demonstrate discrepancies between them. This divergence is explained by the several factors that are the accuracy of calculations for the gyroscope technical data, the accuracy of tests measurement, the drop of the spinning rotor velocity, and variable values of the frictional coefficient in supports and pivot. Nevertheless, the results in tolerance of 10% that accepted in engineering practice for divergence in theoretical and practical results [26]. These data enable for stating that results are well matched and theoretical model for the forces acting on the gyroscope and its motions are satisfied for engineering practice.

The obtained test results are validations of the analytic

statement that the action of the frictional forces on any supports of the gyroscope leads to decreasing the values of the inertial torques. This circumstance leads to increasing the action of the load torque and explain the increasing the angular velocities of precessions. The mathematical model for the forces acting on the gyroscope explains the physics of its motions.

Results and Discussion

The mathematical model for motions around two axes of the gyroscope with one side support developed for the condition of the action of the load and frictional torques on its supports and pivot. The load torques acting on the gyroscope generate several inertial and frictional torques that resulting in gyroscope motions. The action of the frictional torques is manifested in decreasing of the values of the inertial torques. In turn, it leads to increase the action of the load torques that finally expressed in the increase of the angular velocities of the gyroscope motions around two axes. Experimental tests and analytic results for the motions of the gyroscope mounted on the stand are well matched. The mathematical model for motions of the gyroscope with one side support at the condition of the action of load, inertial and frictional torques is validated by practical tests.

Conclusion

The known gyroscope theories in classical mechanics formulated on Euler’s principle of the change in the angular momentum are too simplified and do not much the practical results. For solving the gyroscope problems is derived the numerical modelling of gyroscope effects that produce more or less correct solutions, but cannot explain the physics of processes. New analytic approaches to the gyroscope forces demonstrate that the origin of the problem is more complex than represented in known publications. Actually, gyroscope effects based on the action of the inertial forces that generated by the mass elements and centre mas of the spinning rotor. These forces produce the resistance and precession torques that are interrelated and acted at one time around two axes. Practically, the gyroscopic devices are running with the frictional forces acting on the supports that exert on the gyroscope motions. The experimental tests of the gyroscope with one side support demonstrate that the action of the frictional force increases the angular velocities of the gyroscope around two axes. The mathematical models for the gyroscope motions that based on the new principles explain the physics of gyroscope effects. The new analytic approach to motions of the gyroscope formulated with action of the load, inertial and frictional torques validated by the practical tests.

Appendix

The numerical solution of the case study.

Defined gyroscope parameters that represented in Table 2 as well as in Figure 2 is substituted into the equation of the gyroscope motion around axis *ox* (Equation (24)).

$$2.286976 \cdot 10^{-4} \frac{d\dot{x}}{dt} = (0.146) \cdot (9.81) \cdot (0.0355) + (0.259) \cdot (9.81) \cdot \left[\frac{9\theta 4^2 + 17}{2\theta^2 + 9} \right] \cdot \left(\frac{0.012 + 0.006}{4} \right) \cdot (0.3) - \frac{(0.174) \cdot (9.81) \cdot (0.00424) \cdot (0.1)}{2 \cos 45^\circ} - (4\theta^2 + 17) \cdot (0.5726674 \times 10^{-4}) \cdot (10000) \cdot (2\theta / 60) \dot{x} + \left\{ \left[\frac{9(4\pi^2 + 17)}{2\pi^2 + 9} \right] \cdot \left[\frac{(0.006)0.3}{2} \right] \cdot [1 + (4\pi^2 + 17)^2] - \frac{(0.00424) \cdot (0.1)}{2 \cos 45^\circ} \right\} \cdot (0.146) \cdot (0.0355) \omega_x^2$$

Following simplification and transformation yields the equation:

$$0.0008687 \frac{d\omega_x}{dt} = 0.4216477 - 12.865841\omega_x + \omega_x^2$$

Separating variables and transformation for this differential equation yields the following equation:

$$\frac{d\omega_x}{0.4216477 - 12.865841\omega_x + \omega_x^2} = 1151.1004dt$$

The denominator of the obtained equation is presented as a product of two components that yields the following expression:

$$\frac{d\omega_x}{(\omega_x - 0.0328566) \cdot (\omega_x - 12.832984)} = 1151.1004dt$$

Transformation of the left side of the differential equation into two components yields the following:

$$-\left(\frac{1}{12.800127} \right) \cdot \left(\frac{1}{\omega_x - 0.0328566} - \frac{1}{\omega_x - 12.832984} \right) d\omega_x = 1151.1004dt$$

Transformation and presentation of the obtained equation by the integral form with defined limits yield the following:

$$\int_0^{\omega_x} \frac{1}{\omega_x - 0.0328566} d\omega_x - \int_0^{\omega_x} \frac{1}{\omega_x - 12.832984} d\omega_x = -14734.232 \int_0^t dt$$

Left integrals of the equation are tabulated and represented the integral $\int \frac{dx}{x-a} = \ln x + C$. Right integral is simple. Solving of integrals yields the following equation:

$$\ln(\omega_x - 0.0328566) \Big|_0^{\omega_x} - \ln(\omega_x - 12.832984) \Big|_0^{\omega_x} = -14734.232t$$

giving rise to the following:

$$\omega_x - 0.0328566 = e^{-14734.232t} \cdot (\omega_x - 12.832984)$$

where the right component contains the expression $e^{-14734.232t}$ that has the small value of high order that can be neglected. Hence, the variable angular velocities of the gyroscope precessions are accepted as constant. Then, the theoretical angular velocities of the gyroscope around axes *ox* and *oy* (Equation (3)) are represented by the following result:

$$\omega_x = 0.0328566 \text{ rad / s} = 1.8825449^\circ / \text{s}$$

$$\omega_y = (4\pi^2 + 17)\omega_x = (4\pi^2 + 17) \cdot (1.8825449) = 106.32303^\circ / \text{s}$$

Abbreviations

a, b, b_g, M: Mass of arms, a centre beam, a bar and a gyroscope respectively

d, k : Diameter of a sliding bearing of supports B and D and a thrust bearing of a pivot C respectively

f, f_c : Coefficient of sliding friction at supports and pivot respectively

g : Gravity acceleration

i : Index for axis ox or oy

J : Mass moment of inertia of a rotor's disc

J_i : Mass moment of inertia of a gyroscope around axis i

M : Mass of a rotor's disc

l : Distance between a gyroscope centre mass and a support

R_c : Conditional radius of a rotor

T : Load torque

$T_{am,i}, T_{ct,i}, T_{cr,i}, T_{in,i}$: Torque generated by the change in the angular momentum, centrifugal, Coriolis and common inertial forces respectively, and acting around axis i

$T_{r,i}, T_{pi}$: Resistance and precession torque respectively acting around axis i

T_{fi} : Frictional torque acting around axis i

t : Time

δ : Angle of a cone

γ : Angle of inclination of a spinning axle

η : Coefficient of correction

ω : Angular velocity of a rotor

ω_i : Angular velocity of precession around axis i

References

- Perry J (2012) Spinning Tops and Gyroscopic Motions, Literary Licensing, LLC, NV, USA.
- Cordeiro FJB (2015) The Gyroscope, Createspace, NV, USA.
- Greenhill G (2015) Report on Gyroscopic Theory, Relnk Books, Fallbrook, CA, USA.
- Scarborough JB (2014) The Gyroscope Theory and Applications, Nabu Press, London.
- Neil B (2014) Gyroscope, The Charles Stark Draper Laboratory, Inc., Cambridge, Massachusetts, USA.
- Jonsson RM (2007) Gyroscope precession in special and general relativity from basic principles. American Journal of Physics 75: 463.
- Weinberg H (2011) Gyro Mechanical Performance: the most important parameter. Analog Devices Technical Article MS-2158: 1-5.
- Hibbeler RC, Yap KB (2013) Mechanics for Engineers-Statics and Dynamics, 13th edn. Prentice Hall, Pearson, Singapore.
- Gregory DR (2006) Classical Mechanics, Cambridge University Press, New York.
- Aardema MD (2005) Analytical Dynamics. Theory and Application. Academic/Plenum Publishers, New York.
- Inampudi R, Gordeuk J (2016) Simulation of an Electromechanical Spin Motor System of a Control Moment Gyroscopes. AIAA Guidance, Navigation, and Control Conference.
- Liang WC, Lee SC (2013) Vorticity, gyroscopic precession, and spin-curvature Force. Physical Review D 87: 044024.
- Klein F, Sommerfeld A (2008-2014) The theory of the top Vol. I-IV. Springer, Birkhäuser, New York.
- Zhang N, Ren YF, Li SK (2012) Research on Testing Method of Dynamic Characteristic for MEMS-Gyroscope. Advanced Materials Research 346: 515-520.
- Crassidis JL, Markley FL (2016) Three-Axis Attitude Estimation Using Rate-Integrating Gyroscopes. Journal of Guidance, Control, and Dynamics 39: 1513-1526.
- Gui H, Vukovich G, Xu S (2016) Attitude Stabilization of a Spacecraft with Two Parallel Control Moment Gyroscopes. Journal of Guidance, Control, and Dynamics 39: 728-735.
- Stevenson D, Schaub H (2012) Nonlinear Control Analysis of a Double-Gimbal Variable Speed Control Moment Gyroscopes. Journal of Guidance, Control, and Dynamics 35: 787-793.
- Doupe C, Swenson ED (2016) Optimal Attitude Control of Agile Spacecraft Using Combined Reaction Wheel and Control Moment Gyroscopes Arrays. AIAA Modeling and Simulation Technologies Conference.
- Nanamori Y, Takahashi M (2015) An Integrated Steering Law Considering Biased Loads and Singularity for Control Moment Gyroscopes. AIAA Guidance, Navigation, and Control Conference.
- Braun RD, Putnam ZR, Steinfeldt BA, Grant MJ, Barton G (2013) Advances in Inertial Guidance Technology for Aerospace Systems. AIAA Guidance, Navigation, and Control (GNC) Conference.
- Usubamatov R (2015) Mathematical model for gyroscope effects. AIP Conference Proceedings-American Institute of Physics.
- Usubamatov R (2014) Properties of Gyroscope Motion About One Axis. International Journal of Advancements in Mechanical and Aeronautical Engineering 2: 39-44.
- Usubamatov R (2016) A Mathematical Model for Motions of Gyroscope Suspended from Flexible Cord. Cogent Engineering 3: 1-15.
- Usubamatov R (2017) Mathematical models for principles of gyroscope theory. Proceedings of American Institute of Physics 1798: 020133.
- Usubamatov R, Ismail KA, Sah JM (2014) Analysis of Coriolis Acceleration. Journal of Advanced Science and Engineering Research 4: 1-8.
- Guter RS, Ovchinskii BV (1972) Basis of numerical analysis and mathematical processing of experimental results, Moscow, Nauka.